Journal of Applied Electrochemistry
https://doi.org/10.1007/s10800-023-01849-4

RESEARCH ARTICLE

Reaction pathway of nitrate and ammonia formation in the plasma electrolysis process with nitrogen and oxygen gas injection

Nelson Saksono[1] · Harianingsih[2] · Bening Farawan[3] · Veny Luvita[4] · Zainal Zakaria[5]

Received: 19 October 2022 / Accepted: 2 January 2023

Abstract

The plasma electrolysis method using N_2 and O_2 injection is an effective and environmentally friendly solution for nitrogen fixation into nitrate and ammonia. The reaction pathway, the effect of the N_2 and O_2 gas injection composition are important parameters in understanding the mechanism and effectiveness of these processes. This study aims to determine the formation pathway of nitrate and ammonia by observing the formation and role of reactive species as well as intermediate compounds. Two reaction pathways of NO_x and ammonia formation have been observed. The NO_x compound formed in the solution was oxidized by •OH to NO_2, followed by the production of a stable nitrate compound. The ammonium produced from the ammonia pathway was generated from nitrogen reacting with •H from H_2O. The amount of NH_3 formed was lesser compared to the NO_x compounds in the liquid and gas phases. This indicates that the NO_x pathway is more dominant than that of ammonia. The gas injection test with a ratio of $N_2/O_2 = 79/21$ was the most effective for nitrate formation compared to another ratio. The results of the emission intensity measurement test show that the reactive species •N, •N2*, $•N_2^+$, •OH, and •O have a significant role in the nitrate formation through the NO_x pathway, while the reactive species •N and •H lead to the formation of NH_3. The highest nitrate product was obtained at a ratio of N_2/O_2: 79/21 by 1889 mg L^{-1}, while the highest ammonia product reached 31.5 mg L^{-1} at 100% N_2 injection.

Graphic Abstract

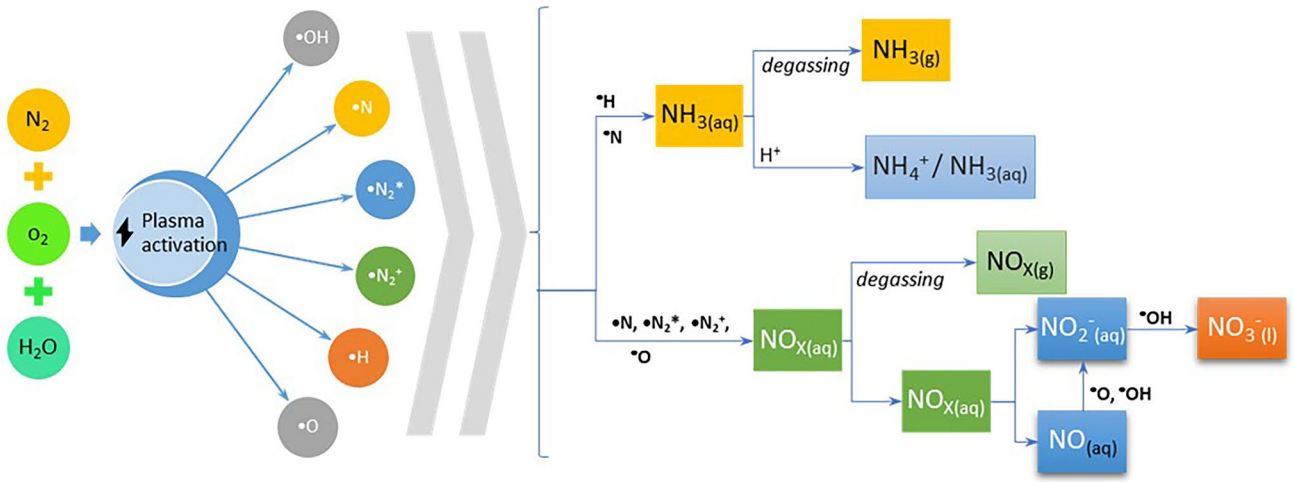

Keywords Ammonia · Plasma electrolysis · Nitrogen fixation · Nitrate · Reactive species

✉ Nelson Saksono
nelsonsaksono@gmail.com

Extended author information available on the last page of the article

Published online: 25 January 2023

1 Introduction

There is about 78% of the nitrogen in the atmosphere is chemically inert which is inaccessible to most organisms. Therefore, it must first be converted to a reactive form (such as ammonia or nitrate) in a process called nitrogen fixation. Industrial nitrogen fixation with the Haber Bosch process can be used to produce nitrogenous fertilizer in the form of ammonia through nitrogen and hydrogen bonding at high temperature and pressure based on reaction Eq. 1 [1].

$$N_2 + 3H_2 \ll 2NH_3 \tag{1}$$

This process occurs at high pressures of 150–200 atm and high temperatures of 500 °C, where the reaction is exothermic with $\Delta H = -92.4$ kJ/mol. It often involves the use of an iron catalyst with K_2O, CaO, SiO_2, and Al_2O_3. Furthermore, a catalyst is very important because the nitrogen (N_2) bond present is included in a very strong triple bond. As a reactant, hydrogen is obtained from natural gas (CH_4) through the steam reforming process based on Eqs. 2 and 3 [2].

$$CH_4 + H_2O \ll CO + H_2 \tag{2}$$

$$CO + H_2O \ll CO_2 + H_2 \tag{3}$$

The Haber Bosch reaction requires energy for the steam reforming process during the conversion of hydrogen gas from natural gas CH_4 along with massive CO_2 emissions [3]. Global NH_3 production capacity is expected to expand to 289.83 million tons in 2030. By 2022, global energy consumption is expected to reach 2–3% of the total production, of global annual energy consumption (18.6 GJ ton NH_3^{-1}), resulting in approximately 235 million tons of CO_2 emissions per year [4]. The increasing demand for fertilizers, high energy use, and environmental concerns caused by emissions from the fixing of N_2 in the current industry has triggered the emergence of a nitrogen fixation process that is sustainable, environmentally friendly, and supports energy savings [5]. Several alternatives have also been studied, such as biological N_2 fixation and nitrogen fixation with metal-complex catalysts at ambient pressure [6]. Another alternative method that has a high potential to reduce environmental impact and increase energy efficiency is Plasma Technology which has proven its application in various important fields such as catalysis [7], energy storage devices [8], and biomedical purposes [9, 10]. Several studies revealed that it can fix free nitrogen (N_2) with O_2 into NO_x compounds with more efficient and environmentally friendly energy (low emission). However, the yield obtained needs to be increased and the product is mostly in the form of gas, which is difficult to further process into fertilizer [11]. Plasma electrolysis technology can successfully overcome the weakness of plasma technology, where the end product of nitrogen fixation is dissolved nitrate liquid with a higher conversion [12, 13].

The technology also combines the principle of plasma formation (ionized gas) and electrolysis reactions in liquid electrolyte solutions. The electrolysis process is carried out at high voltage, forming a gas envelope at one of the anode or cathode poles which in turn triggers the formation of electric sparks due to the excitation of electrons and generation of plasma in the electrolyzed solution [14]. Plasma can produce large amounts of reactive species, which are capable of breaking bonds in H_2O, N_2, and O_2 to form nitrates and ammonia [15]. The process through the injection of air in the zone of an electrolyte solution has been proven to be effective in producing nitrate compounds [14]. It begins with electrolysis, which then leads to the formation of a plasma either in the anode (anodic plasma) or at the cathode (cathodic plasma) as the voltage increases [16]. Plasma electrolysis or also known as contact glow discharge electrolysis (CGDE) can break water molecules into large amounts of •OH and •H [17]. •OH is the strongest oxidizing agent with an oxidation potential of 2.8 eV, while •H acts as the reducing agent. Some H_2O molecules break down into H_2, O_2, and H_2O_2 due to attack from H_2O^+ produced at the anodic plasma [18]. Reactive species •OH, •H, and H_2O^+ diffuse across the plasma layer into the electrolyte stream and then react with each other or the active substrate in the solution [19]. The addition of oxygen and nitrogen molecules to the plasma zone in the plasma electrolysis process has the potential to produce new reactive species in the form of N radicals and O radicals which can form nitrate, nitride, and ammonia compounds through the formation of reactive species.

Injection of N_2 and O_2 gases in the dissolved plasma zone also causes the formation of various reactive species in the form of •OH, •H, •N, and •O based on Eq. 4 [20], Eqs. 5–7 [21]:

$$H_2O_{(g)} + e^- \rightarrow \cdot H + \cdot OH \tag{4}$$

$$N_2 + e^- \rightarrow \cdot N + \cdot N + e^- \tag{5}$$

$$O_2 + e^- \rightarrow \cdot O + \cdot O + e^- \tag{6}$$

$$\cdot O + H_2O_{(l)} \rightarrow \cdot OH + \cdot OH \tag{7}$$

Therefore, this study aims to determine the role of reactive species and their reaction pathways for NO, NO_2, NO_3,

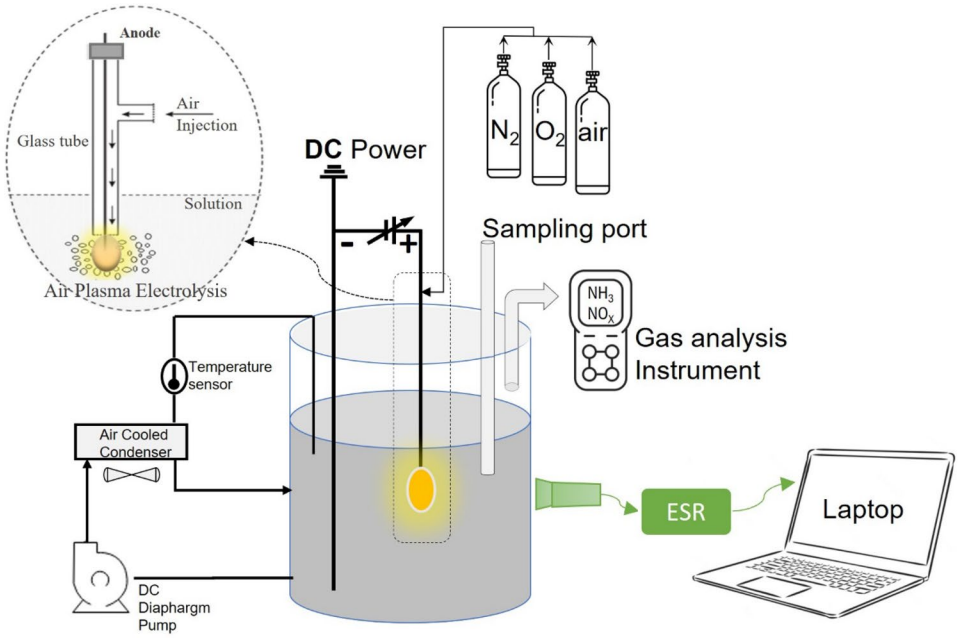

Fig. 1 Scheme of plasma electrolysis reactor

and NH_3 formation in plasma electrolysis through the injection of N_2 and O_2 gases.

2 Methodology

The materials used in this study include nitrogen and oxygen gas, Potassium sulfate MERCK 1.05153.0500 dissolved in distilled water as an electrolyte, and nitrate test reagent HACH 2,106,169. Other materials are a cylindrical reactor made of glass with a volume capacity of 1.2 L as well as a temperature sensor, condenser, power analyzer, AS SUS 316 DIA 5 mm stainless-steel electrode, and tungsten EWTH-2 RHINO GROUND measuring 1.6 mm × 175 mm and powered by a DC power supply. The DC power supply can be set at a voltage of 0–1000 Volts and a current of 0–5 A, as shown in Fig. 1.

The electrolyte solution used was 0.02 M K_2SO_4 with a gas injection flow rate of 0.8 L min^{-1} at a voltage of 700 V and a power of 400 W. Tungsten as an anodic plasma was placed in a glass casing and the length immersed/ contacted in the electrolyte solution at the end of the sheath was 5 mm long (27.13 mm^2 of contact area). The series of experimental tools used in this study were equipped with nitrogen gas cylinders, oxygen, and temperature sensors, limited to 60 °C maximum. Some other tools include test equipment, and a UV VIS spectrophotometer (BEL Engineering UV-M51 Single beam spectrophotometer) to test nitrate, nitrite, and ammonium. Analysis of the intensity of the emission spectrum was carried out with Electron Spin Resonance (ESR) spectroscopy connected to an optical probe in a dark room to determine the gas formed in the reactor due to the presence of plasma discharge at the electrode that occurs. This is due to the release of plasma at the electrodes as well as the removal of other light waves received by the camera. The ESR was tuned at 200–1100 nm with very high UV-NIR response sensitivity using an ICCD (Intensive CCD) camera placed perpendicular to the reactor wall to the plasma source within the closest diameter, where the signal time remained at 1 ms and the output data is processed by the Maya2000 Pro spectrometers application to display semi-qualitative graphical data [22]. The NH_3 gas test was carried out with the AR8500 ammonia sensor, while the NO_x test used the NO_x analyzer ECOM J2KN.

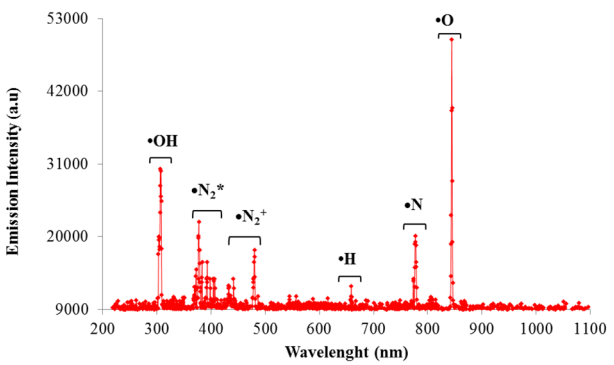

Fig. 2 Emission intensity of reactive species with air injection

3 Findings and discussions

The reaction for the formation of nitrate and ammonia occurs in plasma zone (plasma gas envelope) in the electrolyte solution (Fig. 1), for this reason the discussion begins with observing the formation of reactive species and their products in the liquid phase. Then the compounds produced in the liquid phase can move to the gas phase (above of surface solution) due to certain factors, so that the product compounds are observed in the gas phase. Furthermore, a proposed reaction pathway is made based on observations of reactive species and products. The effect of O_2 and N_2 composition on the formation of reactive species and products is given at the end of this paper.

3.1 Formation of reactive species in the liquid phase

The injection of N_2 and O_2 gases from the air with a flow rate of 0.8 L min^{-1} into the anodic plasma zone in an electrolyte solution of 0.02 M K_2SO_4, a voltage of 700 V, and a power of 400 W proved to be effective in producing several reactive species in the liquid phase, namely •OH, •N, •N_2*, •N_2^+, •H, and •O, as shown in Fig. 2.

Figure 2. shows the light wavelength spectrum of the resulting plasma discharge translated into a graph at 300–850 nm. The wavelengths include: •OH (308 nm), •N_2*(317, 337, 380, 399 nm), •N_2^+ (427, 479 nm), •H (654 nm), •N (777 nm), and •O (844 nm). For emission spectra emitted at various camera positions, the results were dominated by excited nitrogen molecules (•N_2*) due to high-energy collisions of electrons with N_2 and O_2 molecules. Based on the emission spectrum in Fig. 2., •OH, •O, and •H were produced from H_2O molecules in the electrical discharge process through dissociation, ionization, and vibrational excitation/rotation of water molecules [17].

Dissociation

$$H_2O_{(l)} + e^- \rightarrow \cdot OH + \cdot H + e^- \quad (8)$$

Ionization

$$H_2O + e^- \rightarrow 2e^- + H_2O^+ \quad (9)$$

$$H_2O^+ + H_2O \rightarrow \cdot OH + H_3O^+ \quad (10)$$

Excitation

$$H_2O + e^- \rightarrow H_2O^* + e^- \quad (11)$$

$$H_2O^* + H_2O \rightarrow H_2O + \cdot OH + \cdot H \quad (12)$$

$$H_2O^* + H_2O \rightarrow H_2 + \cdot O + H_2O \quad (13)$$

$$H_2O^* + H_2O \rightarrow 2 \cdot H + \cdot O + H_2O \quad (14)$$

H_2O molecules in the gas phase dissociate to form •OH and then diffuse into the solution. Furthermore, the compound split into •OH due to its high-electron energy, which was excited by the plasma. The formation of plasma at the anode in the electrolyte solution changes the chemical effect of the normal electrolysis process, where electron transfer occurs between the ion and the electrode, thereby becoming a non-faraday process [23]. This non-Faraday effect stems from the energy transfer between the high-energy particles in the plasma and other species in the electrolyte near the plasma-liquid interface. It is also obtained from the reactions in the plasma around the anode. These processes increase the number of •OH and •H radicals around the anode in the interfacial region of plasma and electrolyte solutions [24]. •OH can also be generated from the ionization of H_2O molecules by electrons, followed by the reaction of H_2O^+ ions with other H_2O molecules. However, this reaction is unlikely to occur because it requires larger electron energy of 12.6 eV compared to the level needed for H_2O dissociation of 6.4 eV [25]. •OH species have the highest oxidation state, which can oxidize nitrogen from air to nitrate. This species is largely produced by plasma due to gas ionization from the joules heating effect [26]. The high conductivity of 5.4 mS in the 0.02 M K_2SO_4 electrolyte solution led to a more massive release in oxygen bubbles and an increase in the intensity of the O emission. Based on Eq. 15, •O also plays a dominant role in the formation of •OH [27].

$$\cdot O + H_2O_{(l)} \rightarrow \cdot OH + \cdot OH \quad (15)$$

The roles of •N, •N2*, •N2 + , and •O corresponds to Eq. 16 [21], Eq. 17 [28], Eq. 18 [21], Eqs. 19-20 [29].

$$N_2 + e^- \rightarrow \cdot N + \cdot N + e^- \quad (16)$$

$$O_2 + e^- \rightarrow \cdot O + \cdot O + e^- \quad (17)$$

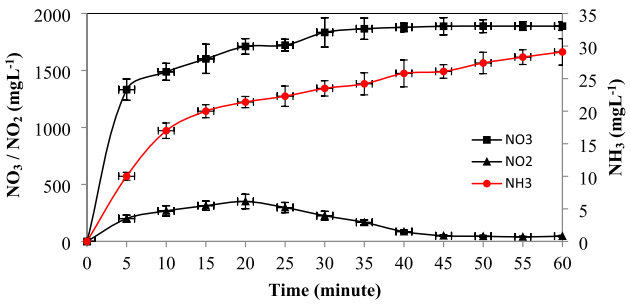

Fig. 3 The concentration of NO_3, NO_2, and NH_3 in the liquid phase

$$N_{2(g)} + H_2O_{(l)} \rightarrow \cdot N_2^+ + \cdot OH + \cdot H \quad (18)$$

$$N_{2(g)} + \cdot O \rightarrow NO + \cdot N_2^* \quad (19)$$

$$\cdot N_2^* + \cdot O \rightarrow NO + \cdot N \quad (20)$$

Species •N, •N_2*, •N_2^+ are generated from N_2 gas activated in the plasma zone, while •O can be obtained from O_2 gas activated by high-energy electrons (e^-). Meanwhile, •OH and •H are formed from the reaction of H_2O with e- from plasma or with •O [27].

3.2 Formation of nitrate, nitrite, and ammonia compounds in the liquid phase

NO_3 was rapidly formed at the beginning of the reaction for up to 35 min. Meanwhile, NO_2 as an intermediate product was rapidly produced for up to 20 min and then decreased again, as shown in Fig. 3. Burlica, et al. [28] stated that the equation for NO_2 formation is through the dissociation reaction of nitrogen and oxygen with the following mechanism.

$$\cdot N_2^* + \cdot O \rightarrow NO_{(g)} \quad (21)$$

$$NO_{(g)} + \cdot O \rightarrow NO_{2(g)} \quad (22)$$

$$3NO_2 + H_2O \rightarrow 2H^+ + 2NO_3^- + NO \quad (23)$$

$$2NO_{2(g)} \rightarrow N_2O_{4(g)} + H_2O_{(L)} \rightarrow HNO_{3(l)} + HNO_{2(l)} \quad (24)$$

$$NO_{2(g)} + NO_{(g)} \rightarrow N_2O_{3(g)} + H_2O_{(l)} \rightarrow 2HNO_{2(l)} \quad (25)$$

$$3HNO_{2(l)} \rightarrow HNO_3 + 2NO_{(g)} + H_2O_{(l)} \quad (26)$$

The NO compounds formed in reactions (23) and (26) can be oxidized to NO_2 when using a gas in the form of air, thereby increasing the concentration of nitrate formed. The reaction between NO_2 and •OH led to the formation of an acid, as shown in the reaction below.

Tabel 1 Ratio of NH_3 and NO_x in gases and liquid phase

Time (minute)	$NH_{3(g)}/NH_{3(l)}$	$NO_{x(g)}/NO_{x(l)}$	Solution's pH
10	0.08	0.172	5.83
30	0.16	0.163	4.41
60	0.17	0.25	3.1

$$NO_2 + \cdot OH \rightarrow HNO_3 \quad (27)$$

Nitrite as an intermediate product formed in this process was oxidized by •OH into more stable nitrate. The production of nitrate, nitrite, and ammonia in the liquid phase is shown in Fig. 3.

Figure 3. shows that the amount of nitrate formed was more than ammonia, the formation of nitrate reaches thousands of ppm, while ammonia is formed around tens of ppm. This condition is due to free Gibbs Energy of nitrate formation (ΔG^o_f -111.3 kJ/mmol), which is much more spontaneous than that of ammonia (ΔG^o_f -26.6 kJ/mmol) under atmospheric conditions. Furthermore, the number of •H species as the main constituent of ammonia (Eq. 28) is much lesser than that of •O species as the main constituent of nitrate, as shown in Fig. 2. Nitrate production increased rapidly in the first 5 min of the reaction and continued until 35 min, after which it tended to be stable until 60 min with a concentration of 1889 mg L^{-1}. This stability can be caused by the decomposition process through exposure to UV light from plasma [30]. The decreasing pH of the solution/acidic (Table 1) during the process also reduced the absorption of NO_2 into NO_3 [14]. Nitrite as an intermediate product increased up to the first 20 min and reached 350.3 mg L^{-1}. It then declined continuously as it was oxidized to nitrate. This decrease also occurs due to air injection and liquid turbulence around the plasma, thereby causing degassing. It also led to the dissolution of NO and NO_2 in the gas to be pushed into the gas phase. Ammonia formed in the liquid phase is in dissolved form and ammonium ions with a concentration of 29.1 mg L^{-1}. The product was formed from nitrogen (•N) and hydrogen (•H) radicals through the dissociation of H_2O [2].

$$\cdot N + \cdot H \rightarrow \cdot NH \quad (28)$$

$$\cdot NH + \cdot H \rightarrow \cdot NH_2 \quad (29)$$

$$\cdot NH_2 + \cdot H \rightarrow \cdot NH_3 \quad (30)$$

3.3 Formation of ammonia and NOx in gas and liquid phases

Plasma-activated Nitrogen, Oxygen, and H_2O gases produce many reactive species in solution and form NO_x as well as NH_3 compounds in the liquid phase. Some of the NO_x and NH_3 products move to the gas phase (above of surface solution) due to several factors, such as degassing, pH of the solution, and exposure to UV light from the plasma. Table 1 presents the ratio of NH_3 and NO_x formed in the liquid and gas phases during the 60 min process.

In the early stages of the process (10 min), NH_3 and NO_x were mostly in the liquid phase (92% for NH_3 and 83% for NO_x), which showed that they were produced in this phase.

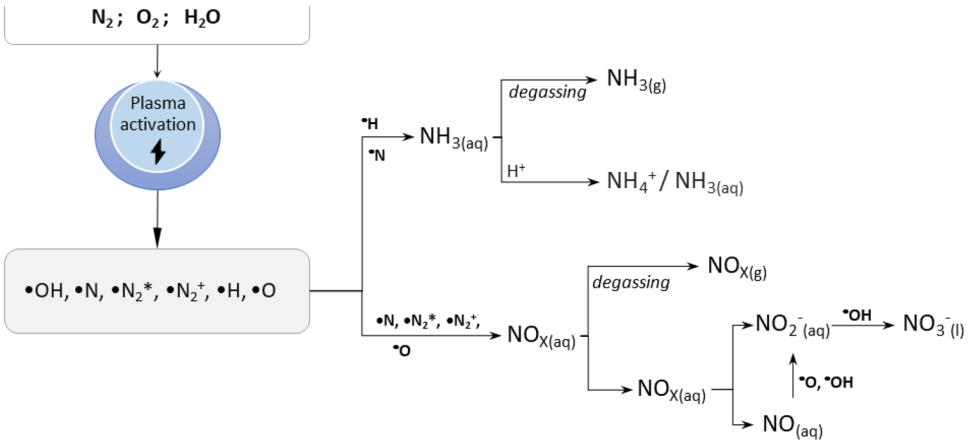

Fig. 4 Pathways of nitrate and ammonia production

Furthermore, the increase in the ratio of $NH_3(g)/NH_3(l)$ and $NO_x(g)/NO_x(l)$ during the 60 min process indicates an increase in the amount of NH_3 and NO_x released into the gas phase from the liquid phase. This was caused by the degassing factor due to the turbulence of fluid around the plasma. The decrease in the pH of the solution during the process due to the formation of nitrate products can also cause an increase in NOx in the gas phase. Activated nitrogen molecules ($•N_2*$) with a low excitation energy level of 6.17 eV can be directly generated by the collision of molecular nitrogen vibrations with electrons. The released N atom then reacts with molecular or atomic oxygen to produce NO_x and with H to form NH_3 [31]. The mole ratio of $NH_3(g)/NH_3(l)$ and $NO_x(g)/NO_x(l)$ products at 60 min reached 0.17 and 0.25, respectively. This indicates that the ammonia formed in the solution was more stable than NO_x. The high ratio of NO_x in the gas phase was due to the low pH of the solution reaching 3.1 at 60 min, thereby reducing the absorption power of NO_2 to NO_3 [14]. UV radiation from plasma can also cause the nitrate formed in the solution to be re-decomposed to NO_x, which later escapes to the gas phase [3]. Increasing the temperature around the plasma during the process can decrease the solubility of NH_3 in the liquid. Consequently, NH_3 moves from the liquid phase to the gas phase, which was indicated by the increasing ratio of NH_3 in the gas phase reaching 0.17 at 60 min.

3.4 Formation pathway of nitrate and ammonia compounds

The dissociation reactions of N_2, O_2, and H_2O that produce reactive species •N, $•N_2*$, $•N_2^+$, •OH, •H, •O, as well as compounds of NO_x and NO_2^- indicate a reaction pathway for the formation of NO_x and Ammonia. The role of each reactive species in the formation is illustrated in Fig. 4.

The NO_x formation pathway occurs due to the injection of N_2 and O_2 gases into the anodic plasma zone. It produces a lot of •O that reacts with •N, $•N_2*$, $•N_2^+$ (Eqs. 16–20) to give $NO_{x(aq)}$ in the solution. Some of the products are released into the gas phase ($NO_{x(g)}$) through the degassing process, while $NO_{x(aq)}$ is oxidized by •O and •OH to NO_2^-(aq) (Eqs. 22–27). Furthermore, the NO_2^-(aq) formed is rapidly oxidized by •OH to a stable nitrate product (NO_3^-). The ammonia reaction pathway occurs due to the reaction of reactive species •H with •N to form ammonia in solution ($NH_{3(aq)}$) (Eqs. 28–30). Some $NH_{3(aq)}$ becomes ammonium ion ($NH_4^+{}_{(aq)}$) after reaction with the acid (H^+) present.

3.5 Effect of N_2 and O_2 composition ratios on formation of reactive species and nitrate-ammonia

The previous discussion revealed the role of reactive species and the reaction pathway for the formation of Ammonia, Nitrate, and Nitrite. Furthermore, this section aims to describe the effect of N_2 and O_2 composition injected into the plasma zone on the number and composition of the reactive species produced. The process was carried out using a semi-quantitative approach with peak intensity absorbance unit (a.u) data.

If plotted as a number, the emission intensities of reactive species from the ESR test results in Fig. 5. are presented in Table 2.

Figure 5. shows that the reactive species •N, $•N_2*$, $•N_2^+$, •OH, •H, and •O occurred at all N_2/O_2 composition ratios except at 100% O_2 ($N_2/O_2 = 0/100$). This was because the ratio did not generate •N, $•N_2*$, and $•N_2^+$ species due to the absence of N_2 injection (Fig. 5f), thereby leading to the absence of nitrate and ammonia products. Figure 5e shows that 100% N_2 ($N_2/O_2 = 100/0$) injection produced the highest •N, $•N_2*$, and $•N_2^+$ indicating that N_2 is effectively activated by plasma, while •OH, •H, and •O were obtained from the dissociation of H_2O molecules. The injection produced the highest N and Ammonia species of 23,148 au and 31.5 mg L^{-1}, respectively, as shown in Table 2. This shows that •N

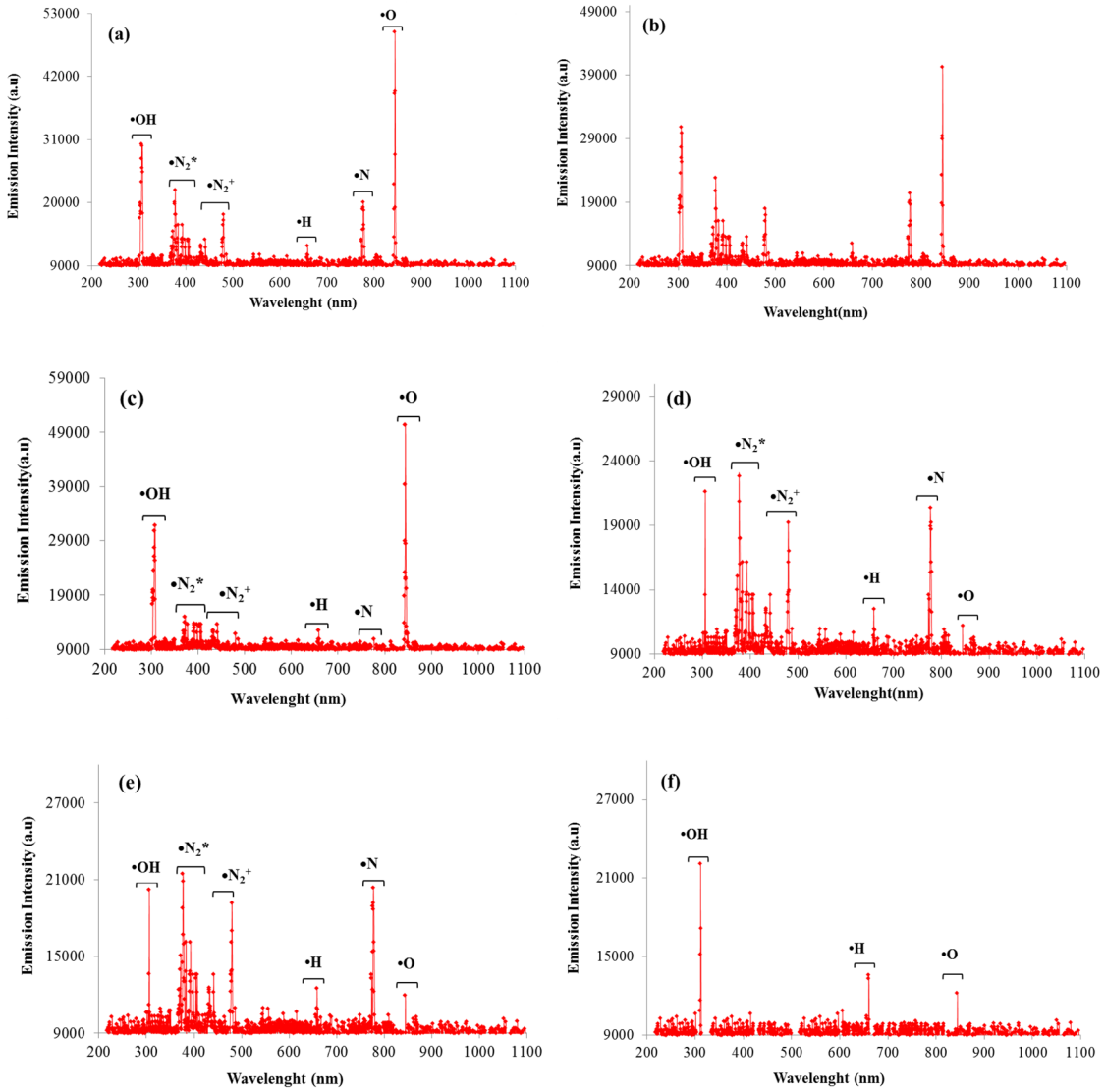

Fig. 5 Emission intensity of species reactive in different ratio composition **a** $N_2/O_2 = 79/21$, **b** $N_2/O_2 = 50/50$, **c** $N_2/O_2 = 20/80$, **d** $N_2/O_2 = 90/10$, **e** 100% N_2, **f** 100% O_2

Table 2 Nitrate, ammonia, and emission intensity of reactive species production in different N_2/O_2 ratio

Ratio	Nitrate**	Ammonia**	Emission intensity of reactive species (a.u)					
	mg L^{-1}	mg L^{-1}	•N	•N_2*	•N_2^+	•OH	•H	•O
$N_2/O_2 = 100/0$	863	31.5	23148	26652	21467	20264	13267	10365
$N_2/O_2 = 90/10$	980	30.3	20984	25991	19212	21677	12798	11214
$N_2/O_2 = 79/21$	1889	29.1	20139	28540	18023	30863	12547	49800
$N_2/O_2 = 50/50$	1702	16.8	20415	25782	22871	30287	12664	40356
$N_2/O_2 = 20/80$	1146	3.9	10211	13651	11889	31890	13213	50402
$N_2/O_2 = 0/100$	–	–	–	–	–	22114	12998	12251

**in 60th minute

species are the main raw material along with •H to form NH_3 (Eqs. 28–30). The low number of N species at $N_2/O_2 = 20/80$, namely 10,211 au only produced 3.9 mg L^{-1} Ammonia, which was much lower than others due to the low •N produced in all ratios.

High •O production occurred at $N_2/O_2 = 79/21$, $N_2/O_2 = 50/50$, and $N_2/O_2 = 20/80$ to produce 49,800 au, 40,356 au, and 50,402, respectively. Meanwhile, at 100% N_2, 100% O_2, and $N_2/O_2 = 90/10$, the amount produced was 10365 au, 12,251 au, and 11,214 au, respectively as shown in Table 2. Injection of N_2 without O_2 was found to produce only low •O, indicating a synergistic role between them. The role of •O is very important in the formation of nitrate through the NO_x pathway (Fig. 4), where high nitrate products are produced at the N_2/O_2 ratio = 79/21. This causes the high production of more •O. •O species play an important role in the formation of $NO_{x(aq)}$, while •OH species is important for oxidizing unstable $NO_{x(aq)}$ to a more stable form of NO_3. Therefore, high •OH produce high Nitrate products, which is influenced by •O species [27], where high •O production will produce high •OH as well, as shown in Table 2. Low •O and •OH products at the ratio of $N_2/O_2 = 90/10$ and 100% N_2 produce low Nitrate products. The highest Nitrate product was achieved at the ratio of $N_2/O_2 = 79/21$ by 1889 mg L^{-1}, as shown in Table 2.

4 Conclusion

This study succeeded in showing the presence of reactive species •N, •N_2*, •N_2^+, •OH, •H, •O, and intermediate compounds NO_x and NO_2^- in the plasma electrolysis process with N_2 and O_2 injection in the anodic plasma zone. The pathway for nitrate formation occurs through the reaction of •N, •N_2*, •N_2^+ with •O to form NO_x and diffuse into the solution. NO_x is oxidized by •OH and •O to form Nitrite as an intermediate product and further oxidized by •OH to Nitrate. The ammonia formation pathway occurs between •N and •H reactive species, with the highest yield achieved at 100% N_2 injection. This ratio also gave the highest Ammonia, namely 31.5 mg L^{-1}. The low formation of •H is the cause of the reduced formation of NH_3 compared to Nitrate. N_2 injection has been proven to increase the formation of reactive species •N, •N_2*, and •N_2^+, while O_2 injection can increase •O and •OH when accompanied by N_2 injection at certain compositions. Injection of N_2 and O_2 at a composition of 79/21 showed the highest •OH and •O with nitrate production of 1889 mg L^{-1}. In future research, the use of cathodic plasma is highly recommended to increase the amount of ammonia.

Acknowledgements The research was partially funded by Publikasi Terindeks International (PUTI) Q2 2022 with contract number NKB-704/UN2.RST/HKP.05.00/2022. The authors declare no competing interest or any conflicts of financial interests

Author contributions Nelson Saksono: Conceptualization, Methodology, Writing - Review & Editing, Project administrationHarianingsih: Conceptualization, Writing - Original DraftBening Farawan: Visualization, data curationVeny Luvita: Data curation, ValidationZainal Zakaria: Supervision, Formal analysis

Funding Publikasi Terindeks International (PUTI),NKB-704/UN2.RST/HKP.05.00/2022,NKB-704/UN2.RST/HKP.05.00/2022

Declarations

Competing interests The authors declare no competing interests.

6. References

1. Patil B, Wang Q, Hessel V, Lang J (2015) Plasma N2-fixation: 1900–2014. Catal Today 256:49–66
2. Rouwenhorst KHR, Krzywda PM, Benes NE, Mul G, Lefferts L (2020) 2020 Ammonia production technologies. Techno-Economic Challenges of Green Ammonia as Energy Vector. Elsevier, Amsterdam, pp 41–84
3. Wang J, Song M, Chen B, Wang L, Zhu R (2017) Effects of pH and H_2O_2 on ammonia, nitrite, and nitrate transformations during UV254nm irradiation: Implications to nitrogen removal and analysis. Chemosphere 184:1003–1011
4. Lee B, Winter LR, Lee H, Lim D, Lim H, Elimelech M (2022) Pathways to a Green Ammonia Future. ACS Energy Lett 7(9):3032–3038. https://doi.org/10.1021/acsenergylett.2c01615
5. Wang Y-Y, Cheng Y-H, Chen K-E, Tsay Y-F (2018) Nitrate transport, signaling, and use efficiency. Annu Rev Plant Biol 69:85–122
6. Cherkasov N, Ibhadon A, Fitzpatrick P (2015) A review of the existing and alternative methods for greener nitrogen fixation. Chem Eng Process 90:24–33
7. Hawtof R, Ghosh S, Guarr E, Xu C, Mohan Sankaran R, Renner JN (2019) Catalyst-free, highly selective synthesis of ammonia from nitrogen and water by a plasma electrolytic system. Sci Adv. https://doi.org/10.1126/sciadv.aat5778
8. Sun J et al (2021) A hybrid plasma electrocatalytic process for sustainable ammonia production. Energy Environ Sci 14(2):865–872. https://doi.org/10.1039/D0EE03769A
9. Al Zoubi W, Kim MJ, Kim YG, Ko YG (2020) Dual-functional crosslinked polymer-inorganic materials for robust electrochemical performance and antibacterial activity. Chem Eng J 392:123654. https://doi.org/10.1016/j.cej.2019.123654
10. Al Zoubi W, Kamil MP, Fatimah S, Nashrah N, Ko YG (2020) Recent advances in hybrid organic-inorganic materials with spatial architecture for state-of-the-art applications. Prog Mater Sci 112:100663. https://doi.org/10.1016/j.pmatsci.2020.100663
11. Wang W, Patil B, Heijkers S, Hessel V, Bogaerts A (2017) Nitrogen fixation by gliding arc plasma: better insight by chemical kinetics modelling. Chemsuschem 10(10):2145–2157
12. Farawan B, Yusharyahya RD, Gozan M, Saksono N (2021) A novel air plasma electrolysis (APE) with direct air injection in plasma zone to produce nitrate in degradation of organic textile dye. Environ Prog Sustain Energy. https://doi.org/10.1002/ep.13691

13. Sharma RK et al (2021) Plasma activated electrochemical ammonia synthesis from nitrogen and water. ACS Energy Lett 6(2):313–319. https://doi.org/10.1021/acsenergylett.0c02349
14. Farisah S, Karamah E, Saksono N (2021) Air plasma electrolysis method for synthesis of liquid nitrate fertilizer with K_2HPO_4 and K_2SO_4 electrolytes. Int J Plasma Environ Sci Technol 15(1):e01005
15. Sakakura T, Takatsuji Y, Morimoto M, Haruyama T (2020) Nitrogen fixation through the plasma/liquid interfacial reaction with controlled conditions of each phase as the reaction locus. Electrochemistry 88(3):190–194
16. Li S, Medrano JA, Hessel V, Gallucci F (2018) Recent progress of plasma-assisted nitrogen fixation research: a review. Processes 6(12):248
17. Jiang B et al (2014) Review on electrical discharge plasma technology for wastewater remediation. Chem Eng J 236:348–368. https://doi.org/10.1016/j.cej.2013.09.090
18. Gao J et al (2008) Degradation of anionic dye eosin by glow discharge electrolysis plasma. Plasma Sci Technol 10:422–427
19. Liu Y, Sun B, Wang L, Wang D (2012) Characteristics of light emission and radicals formed by contact glow discharge electrolysis of an aqueous solution. Plasma Chem Plasma Process 32(2):359–368
20. Bruggeman P et al (2016) Plasma–liquid interactions: a review and roadmap. Plasma Sources Sci Technol 25(5):053002
21. Tsuchida Y, Murakami N, Sakakura T, Takatsuji Y, Haruyama T (2021) Drastically increase in atomic nitrogen production depending on the dielectric constant of beads filled in the discharge space. ACS Omega 6(44):29759–29764
22. Luvita V, Sugiarto A, Bismo S (2022) Characterization of dielectric barrier discharge reactor with nanobubble application for industrial water treatment and depollution. S Afr J Chem Eng 40:246–257
23. Sen Gupta SK (2017) Contact glow discharge electrolysis: a novel tool for manifold applications. Plasma Chem Plasma Process 37(4):897–945. https://doi.org/10.1007/s11090-017-9804-z
24. Sukreni T, Saksono N, Bismo S (2018) Air injection effect on energy consumption and production of hydroxyl radicals at plasma anode. J Environ Sci Technol 12:132–138
25. Lukes P, Locke BR (2005) Plasmachemical oxidation processes in a hybrid gas–liquid electrical discharge reactor. J Phys D Appl Phys 38(22):4074
26. Gupta SKS (2015) Contact glow discharge electrolysis: its origin, plasma diagnostics and non-faradaic chemical effects. Plasma Sources Sci Technol 24(6):063001
27. Yasuoka K, Sato K (2009) Development of repetitive pulsed plasmas in gas bubbles for water treatment. Int J Plasma Environ Sci Technol 3(1):22–27
28. Burlica R, Kirkpatrick MJ, Locke BR (2006) Formation of reactive species in gliding arc discharges with liquid water. J Electrostat 64(1):35–43
29. Chen HH, Chen YK, Chang HC (2012) Evaluation of physicochemical properties of plasma treated brown rice. Food Chem 135(1):74–79
30. Huang L, Li L, Dong W, Liu Y, Hou H (2008) Removal of ammonia by OH radical in aqueous phase. Environ Sci Technol 42(21):8070–8075
31. Chen H, Yuan D, Wu A, Lin X, Li X (2021) Review of low-temperature plasma nitrogen fixation technology. Waste Disposal Sustain Energy 3(3):201–217

Authors and Affiliations

Nelson Saksono[1] · Harianingsih[2] · Bening Farawan[3] · Veny Luvita[4] · Zainal Zakaria[5]

[1] Department of Chemical Engineering, Universitas Indonesia, Kampus Baru UI, Depok 16242, Indonesia

[2] Departemen of Chemical Engineering, Universitas Negeri Semarang, Kampus Sekaran, Semarang 50229, Indonesia

[3] Department of Research and Innovation Infrastructure - BRIN, Cibinong Bogor 16915, Indonesia

[4] Research Centre for Environment and Clean Technology - BRIN, Tangerang Selatan 15314, Indonesia

[5] Pusat Jaminan Kualiti, Universitas Malaysia Sabah, Jalan UMS, Kota Kinibalu, 88400 Sabah, Malaysia

Terms and Conditions

Springer Nature journal content, brought to you courtesy of Springer Nature Customer Service Center GmbH (“Springer Nature”).
Springer Nature supports a reasonable amount of sharing of research papers by authors, subscribers and authorised users (“Users”), for small-scale personal, non-commercial use provided that all copyright, trade and service marks and other proprietary notices are maintained. By accessing, sharing, receiving or otherwise using the Springer Nature journal content you agree to these terms of use (“Terms”). For these purposes, Springer Nature considers academic use (by researchers and students) to be non-commercial.
These Terms are supplementary and will apply in addition to any applicable website terms and conditions, a relevant site licence or a personal subscription. These Terms will prevail over any conflict or ambiguity with regards to the relevant terms, a site licence or a personal subscription (to the extent of the conflict or ambiguity only). For Creative Commons-licensed articles, the terms of the Creative Commons license used will apply.
We collect and use personal data to provide access to the Springer Nature journal content. We may also use these personal data internally within ResearchGate and Springer Nature and as agreed share it, in an anonymised way, for purposes of tracking, analysis and reporting. We will not otherwise disclose your personal data outside the ResearchGate or the Springer Nature group of companies unless we have your permission as detailed in the Privacy Policy.
While Users may use the Springer Nature journal content for small scale, personal non-commercial use, it is important to note that Users may not:

1. use such content for the purpose of providing other users with access on a regular or large scale basis or as a means to circumvent access control;
2. use such content where to do so would be considered a criminal or statutory offence in any jurisdiction, or gives rise to civil liability, or is otherwise unlawful;
3. falsely or misleadingly imply or suggest endorsement, approval , sponsorship, or association unless explicitly agreed to by Springer Nature in writing;
4. use bots or other automated methods to access the content or redirect messages
5. override any security feature or exclusionary protocol; or
6. share the content in order to create substitute for Springer Nature products or services or a systematic database of Springer Nature journal content.

In line with the restriction against commercial use, Springer Nature does not permit the creation of a product or service that creates revenue, royalties, rent or income from our content or its inclusion as part of a paid for service or for other commercial gain. Springer Nature journal content cannot be used for inter-library loans and librarians may not upload Springer Nature journal content on a large scale into their, or any other, institutional repository.
These terms of use are reviewed regularly and may be amended at any time. Springer Nature is not obligated to publish any information or content on this website and may remove it or features or functionality at our sole discretion, at any time with or without notice. Springer Nature may revoke this licence to you at any time and remove access to any copies of the Springer Nature journal content which have been saved.
To the fullest extent permitted by law, Springer Nature makes no warranties, representations or guarantees to Users, either express or implied with respect to the Springer nature journal content and all parties disclaim and waive any implied warranties or warranties imposed by law, including merchantability or fitness for any particular purpose.
Please note that these rights do not automatically extend to content, data or other material published by Springer Nature that may be licensed from third parties.
If you would like to use or distribute our Springer Nature journal content to a wider audience or on a regular basis or in any other manner not expressly permitted by these Terms, please contact Springer Nature at

onlineservice@springernature.com